Journal of Alloys and Compounds 709 (2017) 531–534

Contents lists available at ScienceDirect

Journal of Alloys and Compounds

journal homepage: http://www.elsevier.com/locate/jalcom

# Magnetic viscosity in iron-rhodium nanowires

Julieta S. Riva [a, b, *], Gabriela Pozo-López [a, b, c], Adriana M. Condó [b, d], Jorge M. Levingston [c, e], Luis M. Fabietti [a, b, c], Silvia E. Urreta [c]

[a] Instituto de Física Enrique Gaviola – CONICET, Argentina
[b] Consejo Nacional de Investigaciones Científicas y Técnicas (CONICET), Argentina
[c] Facultad de Matemática, Astronomía y Física, Universidad Nacional de Córdoba, Ciudad Universitaria, 5000, Córdoba, Argentina
[d] Centro Atómico Bariloche, Comisión Nacional de Energía Atómica – Instituto Balseiro, Universidad Nacional de Cuyo, Av. Bustillo 9500, 8400, San Carlos de Bariloche, Argentina
[e] Instituto Nacional de Tecnología Industrial, Centro I+D Formosa, Santa María de Oro 1650, Parque Industrial Formosa, 3600, Formosa, Argentina

ARTICLE INFO

*Article history:*
Received 20 December 2016
Received in revised form
20 February 2017
Accepted 8 March 2017
Available online 9 March 2017

*Keywords:*
Fe-Rh polycrystalline nanowires
Magnetic viscosity
Fluctuations field
Magnetization mechanism

ABSTRACT

Noble/transition bimetallic nanowires of nominal composition $Fe_{90}Rh_{10}$ are AC electrodeposited into 20 nm diameter hexagonally self-assembled alumina nanopores. Nanowires about 18 nm in diameter and 1 μm long are polycrystalline and multiphase. Wires contain α-Fe grains and very small grains of the ClCs-type α′-Fe(Rh) phase. The room temperature magnetization mechanism and the thermal stability of nanowire magnetic configurations are further investigated by measuring the dependence of the coercive field on the applied field sweeping rate R. From these data a mean fluctuations field value of $\mu_0 H_{FR} = (9.0 \pm 0.5)$ mT is obtained (at coercivity) and an effective activation magnetic moment $\mu_{ac} = 5400\ \mu_B$ is estimated, with $\mu_B$ the Bohr magneton. At the coercive field (about 45 mT) the resulting activation lengths become $l_{AC} \approx 6.4$ and 6.7 nm for α-Fe and α′-Fe(Rh), respectively. Assuming an effective magnetic anisotropy, considering magnetostatic shape contributions in addition to the magnetocrystalline one, the domain wall thickness $\delta_w$ in α-Fe grains and in the α′-Fe(Rh) become $\delta_{wFe} = 13.4$ nm and $\delta_{wFeRh} = 10.9$ nm respectively. These values are comparable to the activation lengths estimated at the coercive field in each phase. These facts strongly indicate that irreversible polarization reversal in these nanowires takes place by local curling, involving localized nucleation modes.



## 1. Introduction

In many applications of magnetic nanowires, as magnetic sensors and catalysts [1], the properties of interest are directly related to the stability of a given magnetic state against low and even zero external fields (remanence). Then, the magnetization reversal processes operating in the individual nanowires become of central interest.

Recently, one dimensional bimetallic Fe-rich ($Fe_{90}Rh_{10}$) - nanowires were successfully synthesized by electrodeposition into alumina templates [2], and the resulting microstructures characterized. Nanowires morphology, grain size and phase composition were determined and the magnetic hysteresis properties explored. Special attention was paid to the magnetization reversal mechanism operating in these polycrystalline $Fe_{90}Rh_{10}$ biphasic nanowires by measuring the temperature dependence of the coercive field and the angular variations of coercivity and remanence. The observed behaviors [2] were consistent with a magnetic polarization reversal mechanism controlled by the nucleation of inverse domains by local curling [3]. The apparent activation energy values obtained were comparable to those reported by Paulus et al. (2.4–5.1 eV) [4] for a mechanism of inverse domain nucleation in Fe nanowires. This activation barrier is a measure of the excess in free energy necessary to locally create a domain wall in the nucleation site, determined by factors such as the magnetocrystalline and shape anisotropies, the magnitude of local magnetostatic stray fields and in particular structural defects.

It is then important to provide independent evidence of such localized nucleation to further confirm the mechanism previously proposed, and to estimate the characteristic nucleus size.

In this short article, we report the room temperature values of two magnitudes closely related to the thermally activated polarization reversal mechanism in $Fe_{90}Rh_{10}$ 'as synthesized'

* Corresponding author. Facultad de Matemática, Astronomía y Física, Universidad Nacional de Córdoba, Ciudad Universitaria, 5000, Córdoba, Argentina.
*E-mail address:* jriva@famaf.unc.edu.ar (J.S. Riva).

http://dx.doi.org/10.1016/j.jallcom.2017.03.086
0925-8388/

nanowires: the fluctuations field and the activation volume. The resulting values for these magnitudes strongly support the idea of a magnetization process controlled by the nucleation of inverse domains in quite small regions in the nanowire.

## 2. Experimental procedures

Porous anodized aluminum oxide (AAO) membranes are used as hard templates [5]. The complete procedure to obtain these porous membranes from a high-purity aluminum foil (99.995%, Alfa AEsar) is described elsewhere [2]. Arrays of ordered pores 20 nm in diameter and about 3 μm in length are obtained.

Fe-Rh nanowires are prepared by AC electrodeposition from an aqueous electrolytic bath containing 0.10 M $FeSO_4 \cdot 7H_2O$, 0.0067 M $RhCl_3$, 0.75 g/L ascorbic acid and 30 g/L $H_3BO_3$ in ultrapure water (MilliQ RiOs 16, Millipore), keeping pH = 4.0. Electrodeposition is carried out at room temperature with an AC voltage of 15 $V_{rms}$ and 60 Hz during a few minutes.

XRD profiles are recorded in a PANalytical Empyrean diffractometer, using Cu Kα radiation (λ = 1.5418 Å), in the 2θ range from 30° to 90°. Samples are measured after dissolving the remaining Al substrate in a $CuSO_4$ and HCl solution to eliminate intense Al x-ray peaks. Samples for SEM observations are further immersed in a 1.0 M NaOH solution to dissolve the AAO template and separate the nanowires. After sonication and rinsing in distilled water, dispersed nanowires are obtained, as illustrated in Fig. 1 a.

The nanowire morphology is inspected in a scanning electron microscope FE-SEM Zeiss and the mean array composition determined by energy-dispersive X-ray spectroscopy (EDS), in the SEM. This mean composition is nominal, because nanowires are multiphase, as will be seen below. The individual wire nanostructure and composition are investigated by transmission electron microscopy (TEM) in a Philips CM200UT microscope, operating at 200 kV, with an EDS analysis device. Samples for TEM observations are prepared by dispersing the liberated nanowires in ethanol and further depositing a drop of this emulsion on a holey carbon-coated copper grid.

Room temperature hysteresis loops and polarization relaxation are measured in a vibrating sample magnetometer (VSM) Lakeshore 7300, with a maximum field up to 1.5 T, with the external field applied parallel (PA) and perpendicular (PE) to nanowires major axis. The total magnetic moment of the assembly has contributions from the Al support (paramagnetic), the alumina template (diamagnetic) and the metallic wires filling the pores (ferromagnetic), so the ferromagnetic component must be estimated after subtracting the other contributions.

The hysteresis loops are analyzed considering a linear contribution arising from paramagnetic (Al) and diamagnetic (alumina template) contributions superimposed to a ferromagnetic one, given by Ref. [6]:

$$J_{FM} = \frac{2J_{S,FM}}{\pi} \arctan\left[\frac{(H_i \pm H_{iC})}{H_{iC}} \tan\left(\frac{\pi J_{R,FM}}{2J_{S,FM}}\right)\right], \quad (1)$$

where, $J_{S,FM}$, $\mu_0 H_{iC}$ and $J_{R,FM}$ are the saturation polarization, the coercive field and the remanent polarization, respectively, associated with the ferromagnetic contribution.

The effective fluctuations field $\mu_0 H_{FR}$ [7,8] is determined from the field time rate dependence of the coercive field at constant temperature [9]:

$$H_{FR}(H_i, J) = -\left.\frac{\partial H_i}{\partial \ln R}\right|_J \quad (2)$$

where R is the speed at which the field changes during loop tracing and the internal field: $\mu_0 H_i = \mu_0 H - NJ$, with $H$ the applied field and $N$ the wire demagnetizating factor. Near the coercive field, J~0

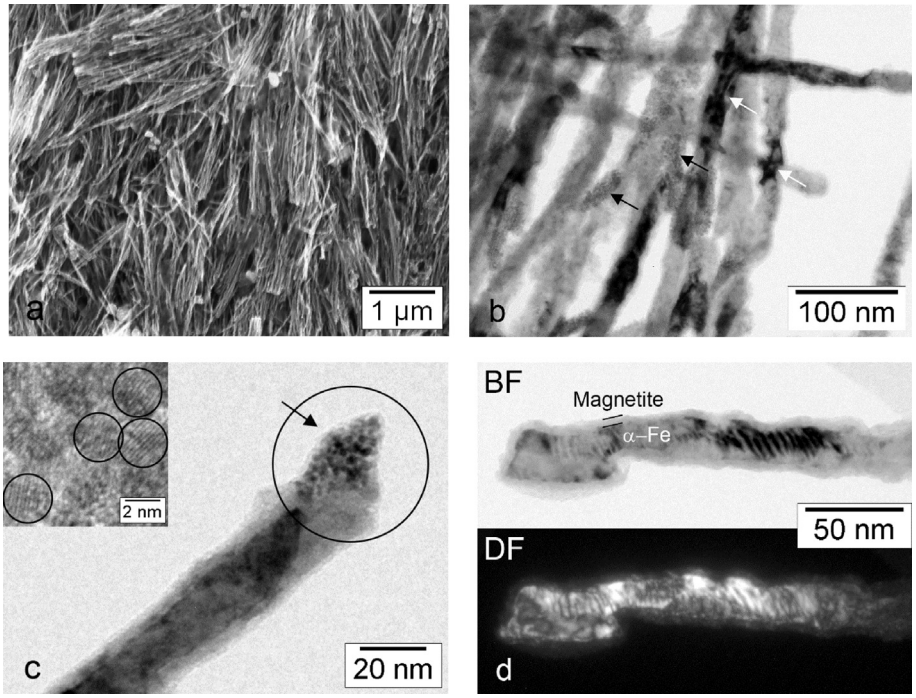


**Fig. 1.** (a) SEM micrograph showing nanowires after partial dissolution of the alumina template. (b) TEM bright field (BF) image of polycrystalline $Fe_{90}Rh_{10}$ nanowires, composed by large α-Fe grains (white arrows) and ensembles of small grains of a Rh-rich ClCs-type phase (black arrows). (c) BF image of small grains of the α′- Fe(Rh) ordered phase at the tip of an α-Fe phase grain (large circle). *Inset*: HRTEM image of the ordered phase, showing very small grains with a mean diameter of (2.0 ± 0.5) nm. (d) Detail of an α-Fe grain: BF micrograph and corresponding 110 dark field (DF) image. A ~4 nm thick magnetite layer is observed at the wire surface.

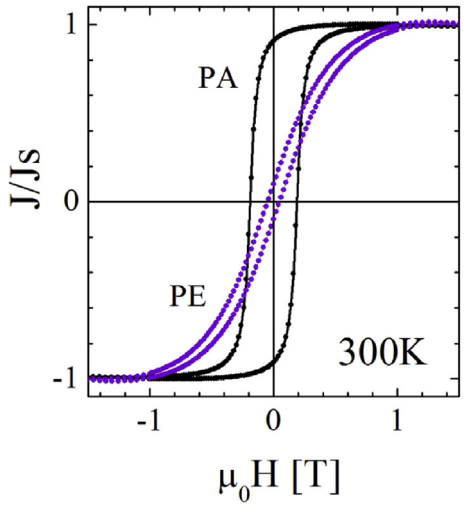


**Fig. 2.** Magnetic hysteresis loops of $Fe_{90}Rh_{10}$ nanowires, measured with the applied field parallel (PA) and perpendicular (PE) to the nanowire major axis. The effect of shape anisotropy is evident.

so the internal field may be approximated in Eqn. (2) by the applied field. The fluctuations field $H_{FR}(H, J)$ is a fictitious field representing the demagnetizing effect of thermal fluctuations at given temperature and applied field values. It is very sensitive to microstructure features and to the actual magnetization mechanism operating in the sample. This fluctuations field may be related to the activation moment $\mu_{ac}$ and the activation volume for polarization reversal $V_{ac}$ by Ref. [8]:

$$\mu_{ac}(H, T) = \frac{k_B T}{\mu_0 H_{FR}(H, J)}. \quad (3)$$

$$V_{ac}(H, T) = \frac{k_B T}{M_S \mu_0 H_{FR}(H, J)}. \quad (4)$$

Here, $k_B$ is the Boltzmann constant, $T$ the absolute temperature and $J_S = \mu_0 M_S$ is the saturation polarization in the region where nucleation takes place.

## 3. Results and discussion

### 3.1. Morphology and microstructure

A detailed structural analysis of $Fe_{90}Rh_{10}$ nanowires has been previously reported in Ref. [2]. SEM and TEM images of $Fe_{90}Rh_{10}$ nanowires (Fig. 1a and b) show that they are about (1.5 ± 0.3) μm long with a mean diameter of (19 ± 1) nm and a quite irregular profile. They are composed of ensembles of very small grains of a Rh-rich phase (black arrows in Fig. 1 b and 1 c) and large Fe-rich grains (Fig. 1 b, white arrows, and d) which are between 100 nm and 1000 nm long. The Rh-rich phase is identified as the ordered α′ phase of the Fe-Rh binary system with a ClCs-type structure [10,11] and has a composition of (42 ± 5) at.% Fe − (58 ± 5) at.% Rh. The mean grain size of this ordered Rh-rich phase is reported to be about (2.0 ± 0.5) nm [2], as can be observed in the HRTEM image shown in the inset of Fig. 1 c. The large Fe-rich grains correspond to the α-Fe phase which has a BCC structure. In Fig. 1 d the BF and DF images of a Fe-rich nanowire show a segment composed of a unique crystal. The nanowire is coated by a (4 ± 1) nm thickness magnetite

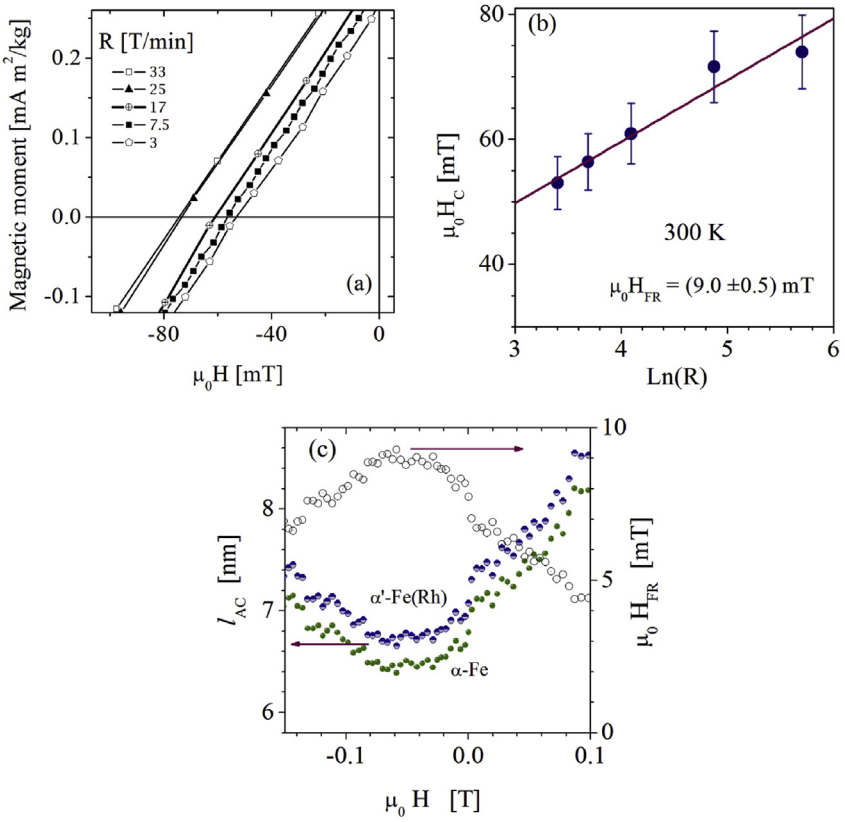


**Fig. 3.** (a) Upper branch of hysteresis loops, near coercivity, corresponding to five different rates R of magnetic field change. (b) Coercive field as a function of the logarithm of field rate R, at the coercive field ($J = 0$); the best linear fit of Eqn. (2) is also shown. (c) Fluctuations field and the corresponding activation lengths as functions of the applied field.

($Fe_3O_4$) layer, with very small grains, likely formed during sample preparation for TEM.

Assuming that the ClCs ordered α'-phase anisotropy is purely magnetocrystalline, of about $K_1 = 1.3 \times 10^4$ J/m$^3$ [12], the room temperature superparamagnetic critic size of this phase becomes $V^*_{SP}\left(=\frac{20\,k_BT}{K_1}\right) \cong 8.6^3 nm^3$, about eighty times larger than the mean grain volume ($2^3$ $nm^3$). If magnetostatic (shape) effects were also considered, an effective uniaxial anisotropy of about $K_U = 58 \times 10^4$ J/m$^3$ may be assumed [2], which leads to a smaller critic volume of about $5.2^3$ nm$^3$, seventeen times larger than the mean grain volume of this phase. From these size considerations a superparamagnetic behavior could be predicted for the α'-phase. However, the small grains of this phase - see Fig. 1 c - are expected to be strongly exchange coupled between them and some of them also coupled to the large neighbor iron grains. In fact, the exchange length $l_{ex}$ is 2.8 nm for Fe and 2.2 nm for the α'-phase so, these small grains are expected to behave more as an exchange coupled 'superferromagnetic-like' phase.

### 3.2. Hysteresis properties and fluctuations field

The room temperature hysteresis loops corresponding to the PA and PE configurations, are displayed in Fig. 2, after subtraction of linear contributions from dia- and paramagnetic phases. The resulting hysteresis loop parameters are coercive fields of 175 mT (PA) and 45 mT (PE), relative remanence of 0.80 (PA) and 0.06 (PE). The saturation polarization, estimated applying the rule of mixtures results 1.95 T.

Besides the free energy barrier, the reversal mechanism is characterized by an apparent activation volume $V_{AC}$. This volume and the room temperature thermally activated nucleation of inverse magnetic domains in $Fe_{90}Rh_{10}$ nanowires are further investigated, by determining the mean fluctuations field. Fig. 3 a shows the upper branch of the hysteresis loops, near coercivity, corresponding to five different rates R of magnetic field change. These loops are measured in the PE condition. A plot of Eqn. (2) near $J = 0$ is depicted in Fig. 3 b together with the best linear fit ($r^2 > 0.94$) leading to a slope value of $\mu_0 H_{FR} = (9.0 \pm 0.5)$ mT. The applied field dependence of the fluctuations field and the associated activation length $l_{AC}(=(V_{AC})^{1/3})$ are shown in Fig. 3 c. As previously indicated these values are better approximations as the applied field approaches to $\mu_0 H_C$ ($J = 0$).

Applying Eqns. (3) and (4) an activation moment $\mu_{ac} = 5400\ \mu_B$ ($\mu_B$ is the Bohr magneton) results. Assuming saturation polarizations of 2.15 T and 1.95 T for α-Fe and for the ordered α′-Fe(Rh) phase respectively, activation lengths may be estimated. These values are plotted in Fig. 3 c together with the fluctuations field, both as functions of the applied field. At the coercive field (about 45 mT) these activation lengths become $l_{AC} \approx 6.4$ and 6.7 nm for α-Fe and α′-Fe(Rh), respectively. These small values are consistent with a polarization mechanism controlled by the localized nucleation of inverse domains as previously proposed, rather than the formation of large vortex and/or transverse domain walls across the entire wire.

Considering magnetic anisotropy values close to the effective ones, $K_U$ [2], and the exchange energy constants $A$ given in Table 1, the domain wall thickness $\delta_w (= \pi \sqrt{A/K_U}$ [13]) in α-Fe grains and in the α′-Fe(Rh) may be estimated. The resulting values, listed in Table 1 are comparable to the activation lengths estimated at the coercive field, considering nucleation at each phase. These results further support our previous conclusions.

**Table 1**
Exchange constant $A$ [13], uniaxial effective crystalline anisotropy $K_U$ [2] and domain wall thickness $\delta w$ corresponding to the relevant magnetic phases in the nanowires.

| | αFe | α′Fe(Rh) |
|---|---|---|
| $A$ [$\times 10^{-11}$ J/m] | 1.5 | 0.7 |
| $K_u \times 10^5$ [J/m$^3$] | 8.2 | 5.8 |
| $\delta w$ [nm] | 13.4 | 10.9 |

## 4. Conclusions

The room temperature fluctuations field in iron-rhodium nanowire arrays of nominal composition $Fe_{90}Rh_{10}$ and 20 nm diameter has been determined. The value corresponding to applied fields near coercivity is $\mu_0 H_{FR} = (9.0 \pm 0.5)$ mT, leading to activation lengths of 6.4 nm and 6.7 nm in the α-Fe and α′-Fe(Rh) phases, respectively. These length values are comparable to domain wall thickness in these phases (13.4 nm and 10.9 nm, respectively) if effective anisotropies, taking account of shape anisotropy are considered. These facts strongly indicate that irreversible polarization reversal in these nanowires involves localized nucleation modes.

## Acknowledgements

Authors thank to Secyt-UNC -Argentine, Program 2016–2017, Res. Secyt 313/16 for financial support.

## References

[1] R.W. Sibin Duan, Bimetallic nanostructures with magnetic and noble metals and their physicochemical applications, Prog. Nat. Sci. Mater. Int. 23 (2013) 113–126.
[2] J.S. Riva, G. Pozo-López, A.M. Condó, M.S. Viqueira, S.E. Urreta, D.R. Cornejo, L.M. Fabietti, Biphasic FeRh nanowires synthesized by AC electrodeposition, J. Alloys Comp. 688 (2016) 804–813.
[3] M.S. Viqueira, N. Bajales, S.E. Urreta, P.G. Bercoff, Magnetization mechanisms in ordered arrays of polycrystalline $Fe_{100-x}Co_x$ nanowires, J. Appl. Phys. 117 (2015) 204302.
[4] P.M. Paulus, F. Luis, M. Kröll, G. Schmid, L.J. de Jongh, Low-temperature study of the mgnetization reversal and magnetic anisotropy of Fe, Ni, and Co nanowires, J. Magn. Magn. Mater. 224 (2001) 180–196.
[5] H. Masuda, K.S. Fukuda, Ordered metal nanohole arrays made by a two-step replication of honeycomb structures of anodic alumina, Science 268 (1995) 1466–1468.
[6] M. Stearns, Y. Cheng, Determination of para and ferromagnetic components of magnetization and magnetoresistance of granular Co/Ag films, J. Appl. Phys. 75 (1994) 6894.
[7] R. Street, J. C Woolley, A study of magnetic viscosity, Proc. Phys. Soc. A 62 (1949) 562.
[8] P. Gaunt, Magnetic viscosity and thermal activation energy, J. Appl. Phys. 59 (1986) 4129.
[9] A. Lyberatos, R. W Chantrell, The fluctuation field of ferromagnetic materials, J. Phys. Condens. Matter 9 (1997) 2623.
[10] L.J. Swartzendruber, ASM Handbook Volume 3: Alloy Phase Diagrams, 1998, p. 853. ISBN 0-87170-381-5 (v.3),23.
[11] H. Okamoto, J. Phase Equilibria Diffusion 32 (5) (2011) 472.
[12] A. Hillion, A. Cavallin, S. Vlaic, A. Tamion, F. Tournus, G. Khadra, J. Dreiser, C. Piamonteze, S. Nolting, S. Rusponi, K. Sato, T.J. Konno, O. Proux, V. Dupuis, H. Brune, Low temperature ferromagnetism in chemically ordered FeRh nanocrystals, Phys. Rev. Lett. 110 (2013) 0872071–0872075.
[13] R.C. O'Handley, Modern Magnetic Materials: Principles and Applications, Edition: 1, John Wiley & Sons Inc, 1 de November 1999. ISBN-10:0471155667.